Compressive and flexural behaviour of recycled aggregate concrete filled steel tubes (RACFST) under short-term loadings

You-Fu Yang[†]

College of Civil Engineering, Fuzhou University, Gongye Road 523,
Fuzhou, Fujian Province 350002, People's Republic of China

Lin-Hai Han[‡]

Department of Civil Engineering, Tsinghua University, Beijing, 100084, People's Republic of China
Key Laboratory of Structural Engineering and Vibration of China Education Ministry, Tsinghua University,
Beijing, 100084, People's Republic of China

Abstract.   The behaviour of hollow structural steel (HSS) stub columns and beams filled with normal concrete and recycled aggregate concrete (RAC) under instantaneous loading was investigated experimentally. A total of 40 specimens, including 30 stub columns and 10 beams, were tested. The main parameters varied in the tests were: (1) recycled coarse aggregate (RCA) replacement ratio, from 0 to 50%, (2) sectional type, circular and square. The main objectives of these tests were threefold: first, to describe a series of tests on new composite columns; second, to analyze the influence of RCA replacement ratio on the compressive and flexural behaviour of recycled aggregate concrete filled steel tubes (RACFST), and finally, to compare the accuracy of the predicted ultimate strength, bending moment capacity and flexural stiffness of the composite specimens by using the recommendations of ACI318-99 (1999), AIJ (1997), AISC-LRFD (1999), BS5400 (1979), DBJ13-51-2003 (2003) and EC4 (1994).

Keywords: recycled aggregate concrete filled steel tubes (RACFST); recycled aggregate concrete (RAC); recycled coarse aggregate (RCA); stub columns; beams; confinement factor; composite actions; member capacity.

1. Introduction

Recycled aggregate concrete (RAC) was introduced into practice many years ago for its ability to solve the increasing waste storage problem and protect the limited natural sources of aggregate (Ajdukiewicz and Kliszczewicz 2002). The RAC refers to the new concrete obtained by partially or completely replacing natural aggregate with recycled aggregate. The recycled aggregate were obtained from crushing, washing, grading and blending according to definite proportions of the crushed concrete

---

†Associate Professor
‡Professor, Corresponding author, E-mail: lhhan@mail.tsinghua.edu.cn

pieces. The research results show that the reuse of waste concrete is feasible, and that RAC is well appreciated in view of its low thermal conductivity, low brittleness as well as low specific gravity that reduces the self-weight of the structures (Katz 2003, Topçu and Şengel 2004). Compared with normal concrete, RAC also has some inherent disadvantages, such as lower strength and modulus, larger shrinkage and creep, weaker durability and higher water infiltration (Katz 2003, Olorunsogo and Padayachee 2002). Xiao *et al*. (2006) review the studies on the structural behaviours of beams, slabs, columns and beam-column connections made from the RAC. The major conclusions by most previous investigators are that the cracking patterns and failure modes of members with RAC are similar to that of the corresponding normal concrete members, but the bearing capacity of RAC elements is a little reduced, however, to an allowable extent. Furthermore, an office building with concrete made from recycled demolition material has been built in Germany. Xiao *et al*. (2006) also present an experimental study on the seismic performance of frame with the RAC. The effects of recycled coarse aggregate (RCA) replacement ratio are emphasized and analyzed in detail. The main conclusions are that the seismic behaviour of the frame with RAC descends with the increasing of RCA replacement percentage. However, the frame with higher RCA contents still behaves well enough to resist the earthquake attack. When the recycled aggregate concrete is deployed in new construction, the consequences of its weakness need to be minimized. Recycled aggregate concrete filled steel tubes (RACFST), which cause the RAC in a state of confinement and protection of outer steel tube, will lower or eliminate the aforementioned weakness of RAC, and lead to full use of the merits of RAC simultaneously. It is thus expected that the RAC will be used in concrete filled steel tubular (CFST) structures in the future because of its good performance. However, the lack of information on the behavior of RACFST indicates a need for further research in this area.

When a thin-walled hollow structural steel (HSS) section is under compression, local buckling may occur if the sectional dimension to thickness ratio (*D/t*) is too high. Filling thin-walled HSS section with concrete to form a composite column is an effective method to avoid local buckling. Furthermore these kind of composite columns have several advantages, such as high load carrying capability, improving the speed of construction, small cross sections for a given column strength over reinforced concrete column, and high fire resistance over steel column (ASCCS 1997). Studies on CFST stub columns and beams have been performed worldwide extensively in the past. Han (2002) and Schneider (1998) reviewed the literature about the research on the behaviour of short CFST columns. Han (2004) and Lu and Kennedy (1994) conducted the review of theoretical and experimental studies on the performance of CFST members subjected to pure bending. Yet there is little literature concerning the compressive and flexural behaviour of RACFST.

Konno *et al*. (1997) studied the behaviour of confined RAC column and normal concrete columns subjected to axial compression. Four specimens were tested. The compressive strength of RAC varied from 30 MPa to 38 MPa, and was 35 MPa for normal concrete. The test results show that the progress of fracture of confined RAC column is faster than that of the confined normal concrete column. However, the new composite column has enough bearing capacity to be utilised though its stiffness and ultimate strength are smaller than those of the confined normal concrete columns. Konno *et al*. (1998) conducted the experimental studies on the strength and the deformation ability of confined RACFST stub columns. Ten specimens were tested, including aforementioned four specimens. The compressive strength of RAC varied from 17.2 MPa to 47.9 MPa, and was from 21.4 MPa to 47.9 MPa for normal concrete. The conclusions were that the deformational behaviour of RACFST was similar to that of CFST and the stiffness of RACFST could be predicted approximately with consideration of the Young's modulus of RAC, which were lower than that of normal concrete.

The present study was an attempt to consider the feasibility of using RAC in HSS columns. The main objectives of this research were threefold: first, to report a series of new tests on HSS stub columns and beams filled with normal concrete and RAC under instantaneous loading, the main parameter in the tests is the RCA replacement ratio (r), second, to analyze the influence of RCA replacement percentage on the behaviour of new composite stub columns and beams, and finally, to compare the accuracy of the predicted ultimate strength, bending moment capacity and flexural stiffness of the composite specimens by using the recommendations of ACI318-99 (1999), AIJ (1997), AISC-LRFD (1999), BS5400 (1979), DBJ13-51-2003 (2003) and EC4 (1994).

Table 1 Specimen labels and member capacities (stub columns)

Section types	No.	Specimen labels	$D \times t$ (mm)	ξ	L (mm)	E_{sc} (×10⁴MPa)		N_{ue} (kN)		ELI (%)	SLI (%)
						Measured value	Average value	Measured value	Average value		
Circular	1	Ca0	○-114×2.19	0.957	342	3.14	3.14	741	741	--	--
	2	Ca1-1	○-114×2.19	0.977		3.09	3.07	700	705.5	2.2	4.8
	3	Ca1-2	○-114×2.19			3.05		711			
	4	Ca2-1	○-114×2.19	1.117		3.01	2.99	674	671.5	4.8	9.4
	5	Ca2-2	○-114×2.19			2.97		669			
	6	Cb0	○-165×2.57	0.784	495	2.94	2.94	1436	1436	--	--
	7	Cb1-1	○-165×2.57	0.800		2.96	2.87	1417	1422	2.4	1.0
	8	Cb1-2	○-165×2.57			2.78		1427			
	9	Cb2-1	○-165×2.57	0.915		2.77	2.77	1401	1401.5	5.8	2.4
	10	Cb2-2	○-165×2.57			2.78		1402			
	11	Cc0	○-219×2.86	0.666	657	2.96	2.96	2158	2158	--	--
	12	Cc1-1	○-219×2.86	0.680		2.87	2.84	2055	2101	4.1	2.6
	13	Cc1-2	○-219×2.86			2.81		2147			
	14	Cc2-1	○-219×2.86	0.777		2.81	2.69	1950	1982	9.1	8.2
	15	Cc2-2	○-219×2.86			2.57		2014			
Square	1	Sa0	□-100×1.94	1.118	300	3.94	3.94	666	666	--	--
	2	Sa1-1	□-100×1.94	1.142		3.82	3.85	645	652.5	2.3	2.0
	3	Sa1-2	□-100×1.94			3.88		660			
	4	Sa2-1	□-100×1.94	1.305		3.79	3.75	624	619	4.8	7.1
	5	Sa2-2	□-100×1.94			3.71		614			
	6	Sb0	□-150×2.94	1.003	450	3.48	3.48	1306	1306	--	--
	7	Sb1-1	□-150×2.94	1.024		3.40	3.39	1279	1283	2.6	1.8
	8	Sb1-2	□-150×2.94			3.38		1287			
	9	Sb2-1	□-150×2.94	1.170		3.32	3.29	1250	1271.5	5.5	2.6
	10	Sb2-2	□-150×2.94			3.26		1293			
	11	Sc0	□-200×3.73	0.912	600	2.78	2.78	2295	2295	--	--
	12	Sc1-1	□-200×3.73	0.931		2.62	2.63	2123	2180.5	5.4	5.0
	13	Sc1-2	□-200×3.73			2.63		2238			
	14	Sc2-1	□-200×3.73	1.064		2.51	2.54	2098	2119	8.6	7.7
	15	Sc2-2	□-200×3.73			2.57		2140			

Table 2 Specimen labels and member capacities (beams)

Section types	No.	Specimen labels	D×t (mm)	ξ	L (mm)	K_{ie} (kN.m²) Measured value	K_{ie} (kN.m²) Average value	K_{se} (kN.m²) Measured value	K_{se} (kN.m²) Average value	M_{ue} (kN.m) Measured value	M_{ue} (kN.m) Average value	SLI_i (%)	SLI_s (%)	MLI (%)
Circular	1	BCb0	○-165×2.57	0.784		1386.4	1386.4	1259.3	1259.3	29.4	29.4	--	--	--
	2	BCb1-1	○-165×2.57	0.800	1200	1335.3	1341.2	1219.8	1220.7	28.2	28.15	3.3	3.1	3.5
	3	BCb1-2	○-165×2.57			1347.1		1221.6		28.1				
	4	BCb2-1	○-165×2.57	0.915		1270.3	1266.2	1163.1	1160.5	27.8	27.65	8.7	7.8	6.3
	5	BCb2-2	○-165×2.57			1262.1		1157.9		27.5				
Square	1	BSb0	□-150×2.94	1.003		1971.3	1971.3	1850.9	1850.9	34.9	34.9	--	--	--
	2	BSb1-1	□-150×2.94	1.024	1200	1911.5	1903.8	1801.5	1790.3	33.6	33.8	3.4	3.3	3.9
	3	BSb1-2	□-150×2.94			1896.1		1779.1		34.0				
	4	BSb2-1	□-150×2.94	1.170		1798.5	1804.9	1702.3	1698.9	32.9	33	8.4	8.2	8.1
	5	BSb2-2	□-150×2.94			1811.3		1695.5		33.1				

2. Experimental program

Forty specimens, including thirty stub columns and ten beams, were tested in this study. The main parameters varied in the tests were: (1) column section types, circular and square, and (2) RCA replacement ratio r (i.e., the ratio of RCA mass to the mass of all coarse aggregate), which was 0%, 25% and 50%, and for normal concrete, RCA replacement ratio was equal to zero, which was designed as the reference concrete for comparison purposes. A summary of the specimens was presented in Table 1 and 2. The main experimental parameters were listed below, along with the labels used to characterize each specimen:
- Section type (C = circular, S = square);
- Dimension (a: Diameter = 114 mm or width = 100 mm, b: Diameter = 165 mm or width = 150 mm, c: Diameter = 219 mm or width = 200 mm);
- Filled concrete type (0 = normal concrete, 1 = RAC containing 25% RCA, 2 = RAC containing 50% RCA);
- "B" is designated for beam specimens.

For example, the specimen beginning with the label "Cb1-1" would be the first circular composite columns filled with RAC containing 25% RCA, and its diameter is 165 mm.

(a) Concrete filled CHS   (b) Concrete filled SHS
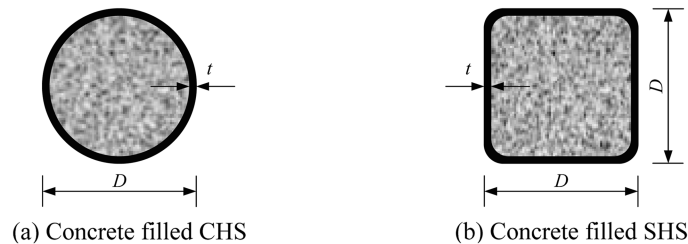
Fig. 1 Cross-sectional dimensions of test specimens

Table 3 Steel properties

Steel section	Dimension of section $D{\times}t$ (mm)	Yield strength f_{sy} (MPa)	Tensile strength f_u (N/mm^2)	Yield ratio Y (f_{sy}/f_u)	Modulus of elasticity E_s (N/mm^2)	Poisson's ratio μ
Circular	○-114×2.19	335.7	435.8	0.77	1.95×10^5	0.272
	○-165×2.57	343.1	423.6	0.81	1.79×10^5	0.277
	○-219×2.86	350.4	465.8	0.75	1.81×10^5	0.288
Square	□-100×1.94	388.1	495.7	0.78	1.93×10^5	0.291
	□-150×2.94	344.4	450.5	0.76	2.07×10^5	0.292
	□-200×3.73	330.1	463.5	0.71	2.06×10^5	0.278

Table 4 The properties of NCA and RCA

Type	Grading (mm)	Bulk density (kg/m^3)	Unit weight (kg/m^3)	Water absorption (%)	Crushing value (%)
NCA	5-16	1420	2600	0.42	15.3
RCA	5-26.5	1260	2470	8.43	19.7

Table 5 The mix proportions and properties of concrete

Type of concrete	r (%)	Cement (kg/m^3)	Sand (kg/m^3)	NCA (kg/m^3)	RCA (kg/m^3)	Water (kg/m^3)	W/C	Compressive mean cube strength, $f_{cm,cube}$ (MPa)	Modulus of elasticity, E_c (MPa)
Normal concrete	0	414	630	1170	0	207	0.5	42.7	2.75×10^4
Recycled aggregate concrete	25	414	630	878	292	207	0.5	41.8	2.61×10^4
	50	414	630	585	585	207	0.5	36.6	2.46×10^4

Fig. 1 shows the cross sections of the test specimens, where D is the outside diameter or width of the steel tube with circular or square sections respectively; t is the wall thickness of circular steel tube or the flat part of square steel tube.

Strips of the steel tubes were tested in tension. Three coupons were taken from each type of the steel tube. The 0.2% proof stress was adopted as the yield strength. From these tests, the average yield strength (f_{sy}), tensile strength (f_u), yield ratio (f_{sy}/f_u), modulus of elasticity (E_s) and Poisson's ratio (μ) of the steel tubes were listed in Table 3.

Three different concrete mixes were used. The mix was designed for compressive mean cube strength ($f_{cm,cube}$) at 28 days of approximately 40 MPa. In producing RAC, in place of natural coarse aggregate (NCA), portions of 25% and 50% RCA were added as coarse aggregate. RCA were obtained by crushing waste concrete, which taken from failure CFST joint and plane frame specimens, and sieving with a mesh square of 26.5 mm (5-16 mm is 55% and 16-26.5 mm is 45% in weight). The compressive mean cube strength of the waste concrete was about 50 MPa and the coarse aggregate was the same as the NCA used in this study. The physical properties of NCA and RCA were given detail in Table 4.

All specimens were cast from one batch of concrete. Several 150 mm cubes and 150 mm×300 mm prisms were also cast and cured in conditions similar to the corresponding specimens.

The mix proportions and properties of the concrete were summarized in Table 5. The stress-strain relationships of three different concretes were shown in Fig. 2 (only ascending curves were measured
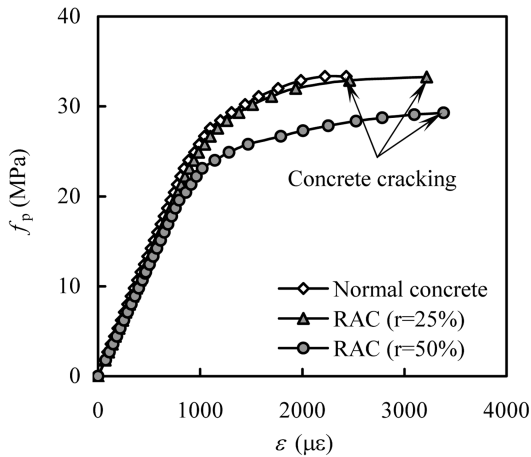
Fig. 2 Stress-strain relationships of different concrete
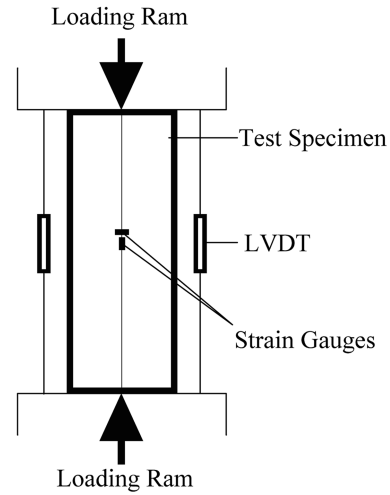
Fig. 3 Layout of stub column test

due to the cracking of concrete), where f_p was the prism strength of concrete. It could be seen that the strength and elastic modulus of RAC were lower than those of normal concrete, and the higher the RCA replacement ratio was, the lower the strength and elastic modulus were. It also could be found from Fig. 2 that the strain corresponding to the maximum strength of RAC is larger than that of normal concrete.

In all the concrete mixes, the fine aggregate used was silica-based sand and the normal concrete was carbonate stone from Fuzhou City, South of China.

The tubes were all manufactured from cold-formed HSS sections. The ends of the steel tubes were cut and machined to the required length. The insides of the tubes were wire brushed to remove any rust and loose debris present. Each tube was welded to a circualr (for circular sections) or sqaure (for sqaure sections) steel base plate 16 mm thick. The specimens were placed upright to air-dry until testing occurred. During curing, a very small amount of longitudinal shrinkage of 0.4 to 1.0 mm or so occurred at the top of the column. A high-strength epoxy was used to fill this longitudinal gap so that the concrete surface was flush with the steel tube at the top.

The experimental study was to determine not only the maximum bearing capacity of the specimens, but also to investigate the failure pattern up to and beyond the ultimate load. The experimental program consisted of two stages, which were described below and designated type I and II.

2.1. Type I: Stub column tests

A total of thirty stub specimens were tested. A summary of the specimens was presented in Table 1. The length of stub columns (L) was chosen to be three times the diameter (for circular specimens) or the width (for square specimens) to avoid the effects of overall buckling and end conditions (Han *et al.* 2001).

All the tests were performed on a 5000 kN capacity testing machine. The specimens were placed in the testing machine and the loads were applied on the specimens directly. Fig. 3 gives a schematic view of the test arrangement. The loading ram was a solid steel plate, which acted like an end stiffener. The specimens were adjusted for verticality to avoid any initial inclination before the testing. Eight strain

gauges were used for each specimen to measure strains at the mid-height. Two linear voltage displacement transducers (LVDTs) were used to measure the axial deformation, shown in Fig. 3. A load interval of less than one tenth of the estimated load capacity was used. Each load interval was maintained for about 2 to 3 minutes.
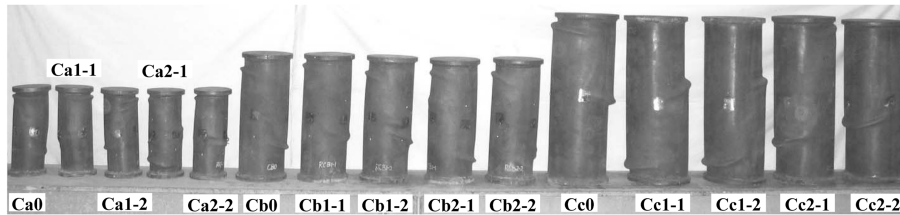
(a) Concrete filled CHS

(b) Concrete filled SHS

Fig. 4 Failure modes of stub columns
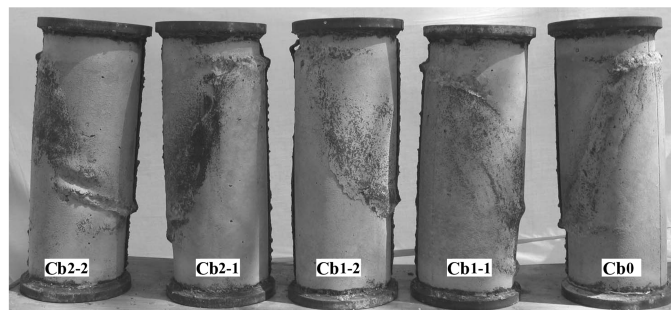
(a) Concrete filled CHS

(b) Concrete filled SHS

Fig. 5 Typical failure modes of core concrete in stub columns

From the tests, it was found that all specimens show relatively good ductility and post-peak bearing capacity. The test proceeded in a smooth and controlled fashion, and the RCA replacement ratio almost had no influence on the failure pattern up to and beyond the ultimate strength. The specimens were in elastic stage initially, and when the applied loads reached 60~70 percentage of the ultimate strength, slip lines appeared at local of the steel tube. As loading continued further, the slip lines increased with
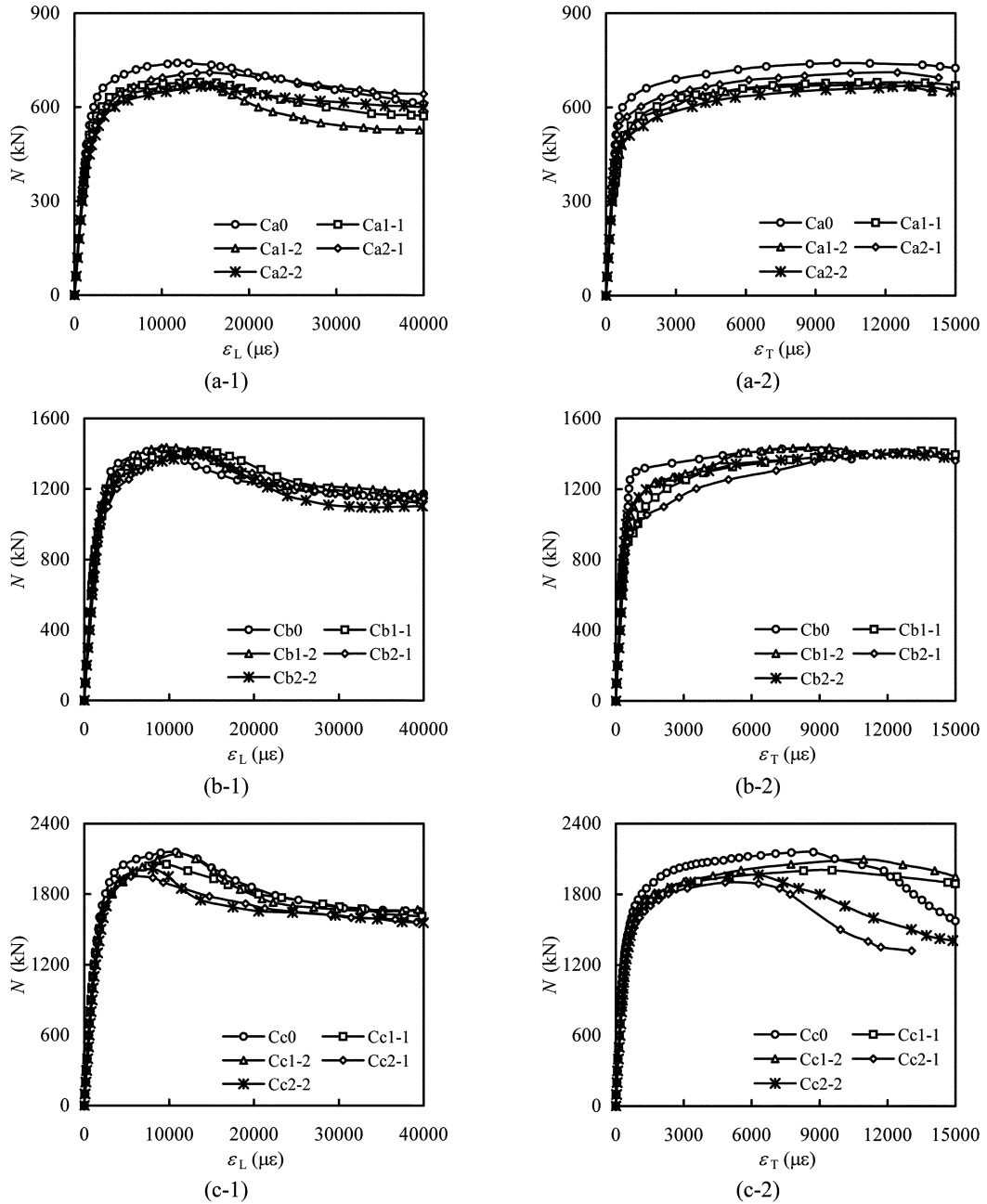
Fig. 6 Axial load (N) versus axial strain (ε) curves (circular sections)
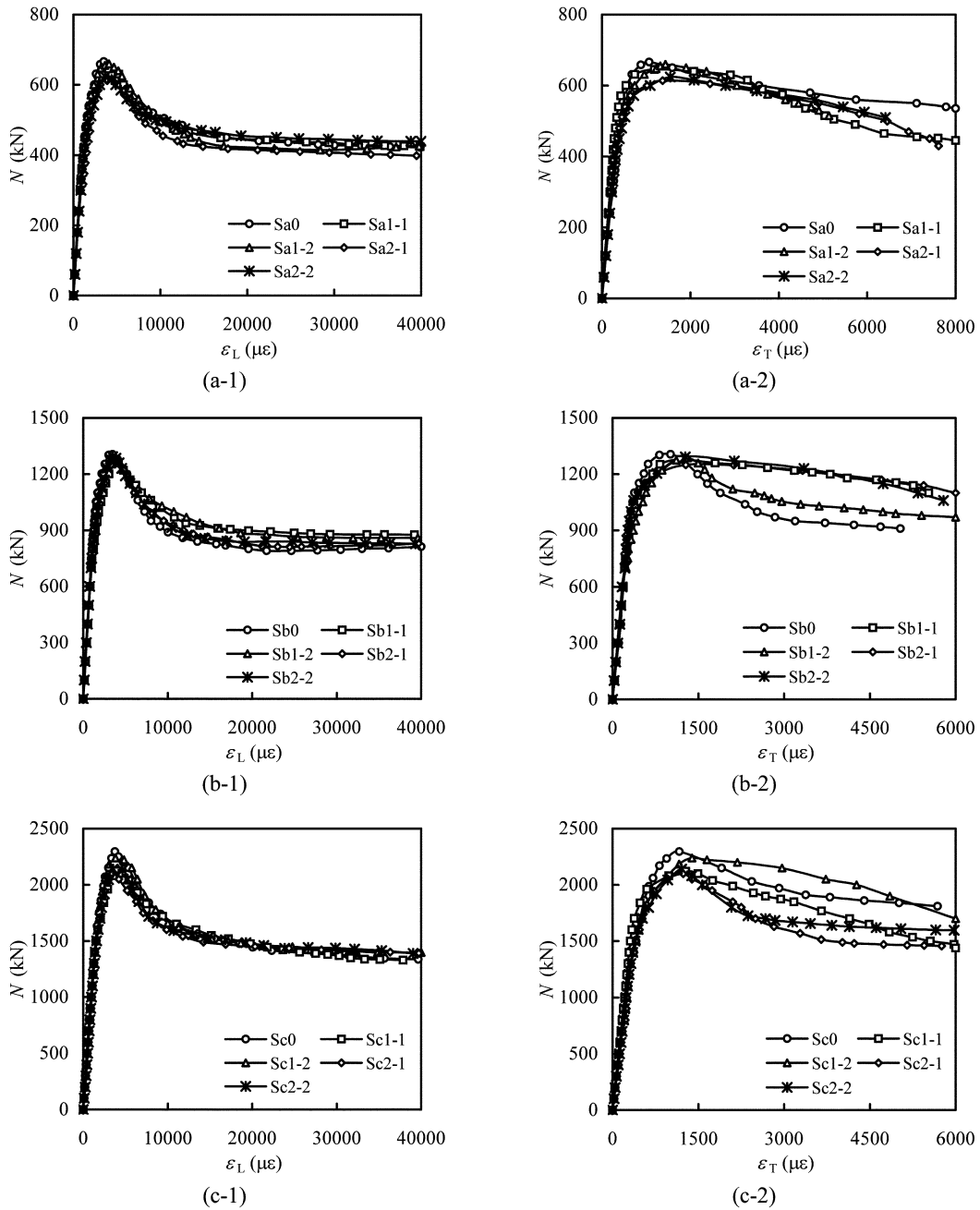
Fig. 7 Axial load (N) versus axial strain (ε) curves (square sections)

the increasing of applied loads, and gradually distributed fully through the steel tube, then the specimens come into failure stage. Because the confinement factor ξ ($=\dfrac{A_s \cdot f_{sy}}{A_c \cdot f_{ck,cube}}$) of all circular specimens is relatively low, i.e., the steel tube can't provide adequate confinement for core concrete, and the failure mode of circular specimens is shear type. For square specimens, typical failure modes of

Table 6 Relationship between longitudinal and transverse strain of stub columns

Section types	No.	Specimen	ε_L ($\times 10^{-6}$)	ε_T ($\times 10^{-6}$)	Strain ratio ($\varepsilon_T / \varepsilon_L$)
Circular	1	Ca0	11788	9909	0.84
	2	Ca1-1	14403	11637	0.81
	3	Ca1-2	13675	11469	0.84
	4	Ca2-1	15496	12504	0.81
	5	Ca2-2	15570	12999	0.83
	6	Cb0	9160	7345	0.80
	7	Cb1-1	11399	10492	0.92
	8	Cb1-2	9682	8493	0.88
	9	Cb2-1	12340	11079	0.90
	10	Cb2-2	13518	12605	0.93
	11	Cc0	10816	8735	0.81
	12	Cc1-1	10686	9549	0.89
	13	Cc1-2	11153	9954	0.89
	14	Cc2-1	5508	4827	0.88
	15	Cc2-2	8096	6294	0.78
Square	1	Sa0	3493	1069	0.31
	2	Sa1-1	4046	1184	0.29
	3	Sa1-2	4106	1435	0.35
	4	Sa2-1	3767	1369	0.36
	5	Sa2-2	3656	1548	0.42
	6	Sb0	3467	1013	0.29
	7	Sb1-1	3827	1177	0.31
	8	Sb1-2	3694	1314	0.36
	9	Sb2-1	3595	1281	0.36
	10	Sb2-2	3484	1271	0.36
	11	Sc0	3370	1169	0.35
	12	Sc1-1	4006	1282	0.32
	13	Sc1-2	3813	1390	0.36
	14	Sc2-1	3440	1235	0.36
	15	Sc2-2	3553	1210	0.34

the outer steel tube are local (outward folding) failure mechanism, and this is the same as that observed by many other researchers, such as Han *et al.* (2001), Uy (2000) etc. The failure modes of stub columns with different RCA replacement ratio and sectional dimension are shown in Fig. 4. Fig. 5 shows typical failure modes of concrete core in stub columns.

Total of the tested curves of axial load (N) versus axial strain (ε_L and ε_T) are shown in Figs. 6 and 7 for specimens with circular and square sections respectively, in which ε_L is the longitudinal strain and ε_T is the transverse strain. The elastic modulus (E_{sc}) and ultimate strengths (N_{ue}) obtained in the test are summarised in Table 1. It can be seen that E_{sc} and N_{ue} decrease with an increase of RCA replacement ratio.

(a) Ca series

(b) Cb series

(c) Cb series
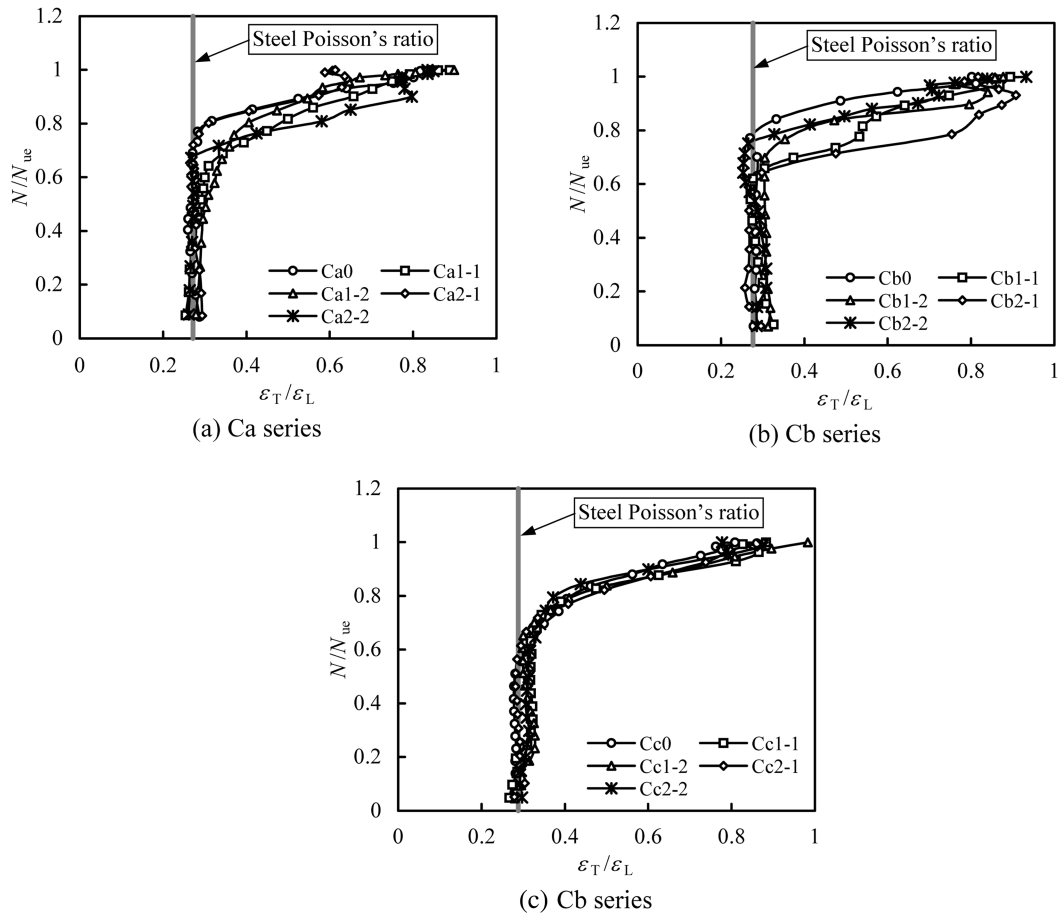
Fig. 8 Relationships of load ratio (N/N_{ue}) versus strain ratio ($\varepsilon_T/\varepsilon_L$) (circular sections)

The longitudinal and transverse strains and the strain ratio ($\varepsilon_T/\varepsilon_L$) at the ultimate load are listed in Table 6. It can be seen that, in general, the strain (ε_L and ε_T) of the specimens with RAC is larger than that of the specimens with normal concrete. The strain ratio ranges from 0.78 to 0.93 for circular specimens and 0.29 to 0.42 for square specimens. Figs. 8 and 9 depict the relationships of load ratio (N/N_{ue}) versus strain ratio ($\varepsilon_T/\varepsilon_L$). It can be seen that, for circular specimens, when the load ratio approaches 0.6 to 0.7, the strain ratio begins to exceed the steel Poisson's ratio. However, for square specimens, the load ratio is 0.9 and even higher. It means that the "composite action" between the steel tube and core concrete of circular specimens occurs earlier than that of square specimens, and the constraining effect to core concrete of circular steel tube is better than that of square steel tube (ASCCS 1997).

2.2. Type II: Beam tests

A total of ten beam specimens with circular and square sections were tested. A summary of the specimens was presented in Table 2. The specimens were designed with different concrete type

(a) Sa series

(b) Sb series

(c) Sc series
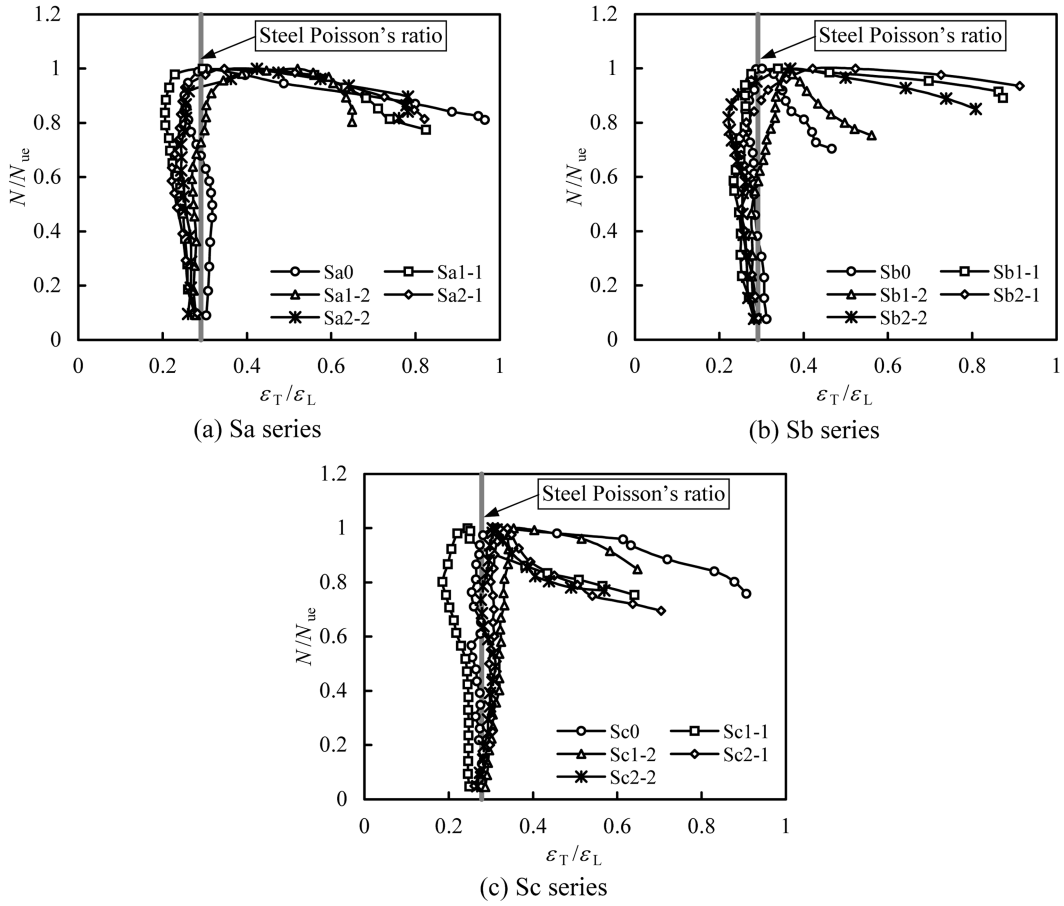
Fig. 9 Relationships of load ratio (N/N_{ue}) versus strain ratio ($\varepsilon_T/\varepsilon_L$) (square sections)
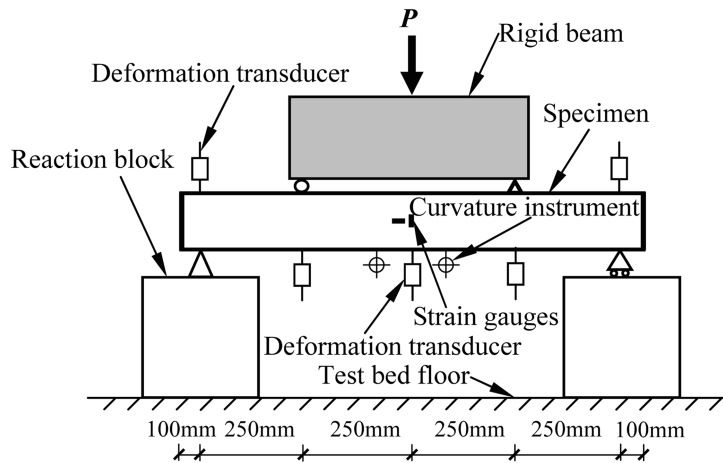
Fig. 10 Arrangement of beam test

(a) Concrete filled CHS   (b) Concrete filled SHS
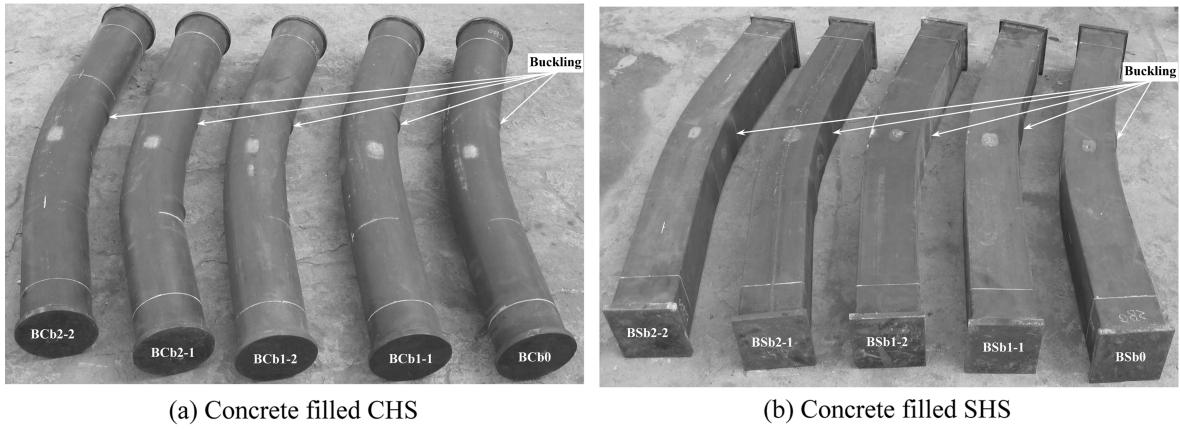
Fig. 11 Failure modes of tested beams

(a) Concrete filled CHS

(b) Concrete filled SHS
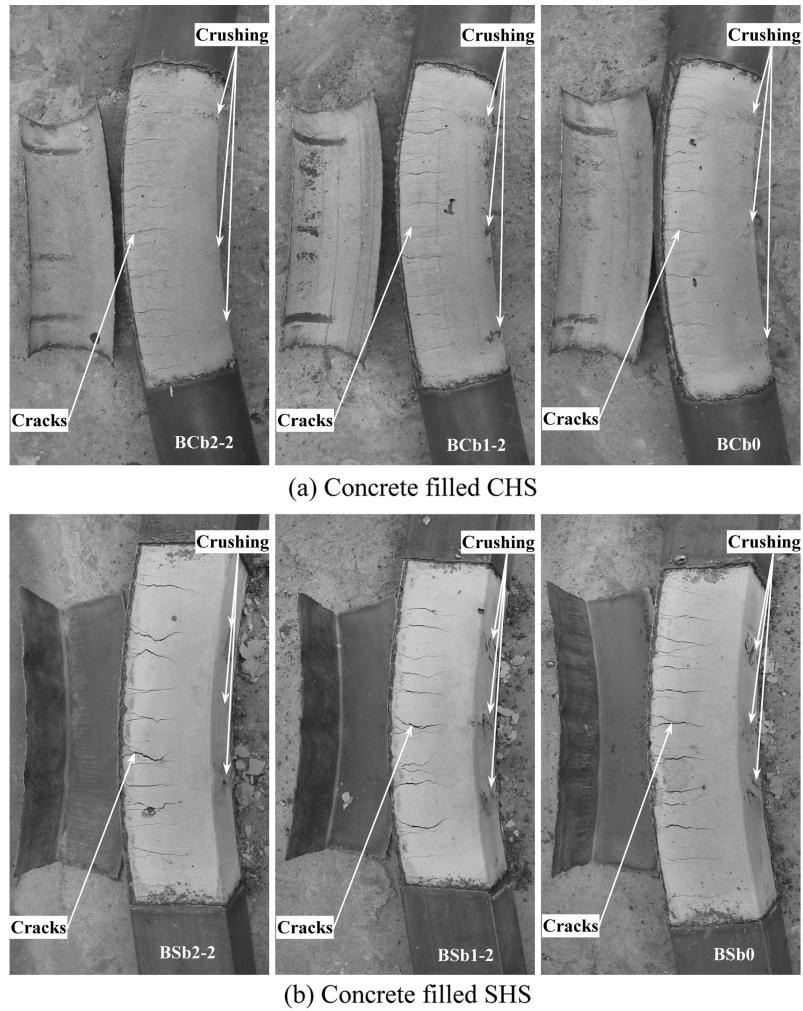
Fig. 12 Typical failure modes of core concrete in beams

(including normal concrete and RAC) being achieved. The tube depth to wall thickness ratio (D/t) was 64 and 51 for circular specimens and square specimens respectively. All specimens were 1200 mm in length.

A four point bending rig was used to apply the moment (see Fig. 10). The in-plane displacements were measured at locations along the specimen bottom by three displacement transducers. Two curvature instruments were placed near the mid-span to measure the curvatures, and eight strain gauges were used for each specimen to measure strains at the mid-span. A load interval of less than one-tenth of the estimated load capacity was used. Each load interval was maintained for about 2-3 min. At each load increment, the strain readings and the deformation measurements were recorded. All specimens were loaded to failure.

The test results show that the failure modes of all beam specimens are almost same, and the effect of RCA replacement ratio is very small. The tested specimens failed in a very ductile manner and no tensile fracture is observed on the tension zone. Typical failure modes are shown in Figs. 11 and 12. It can be seen that the failure mode of the steel tube involves several local buckles in the compression
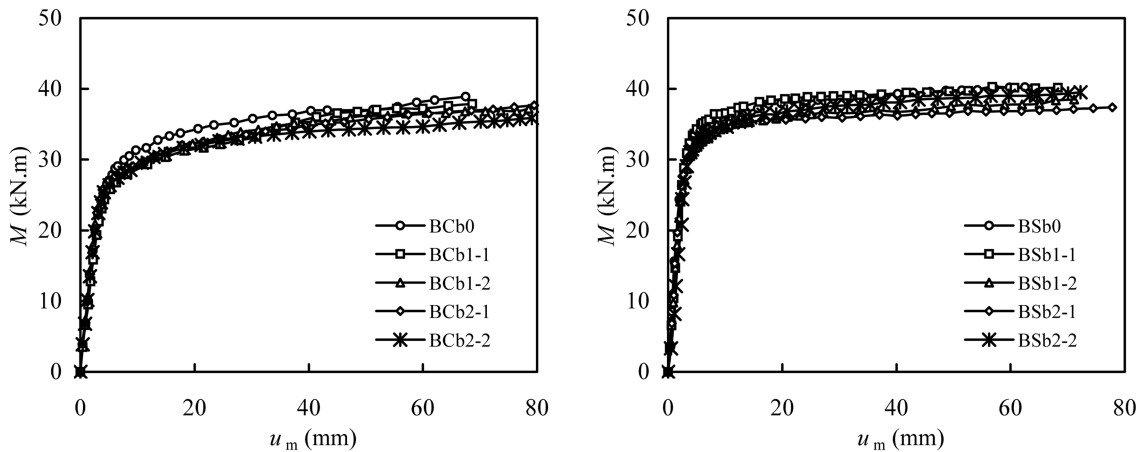
Fig. 13 Moment (M) versus mid-span deflection (u_m) relationships
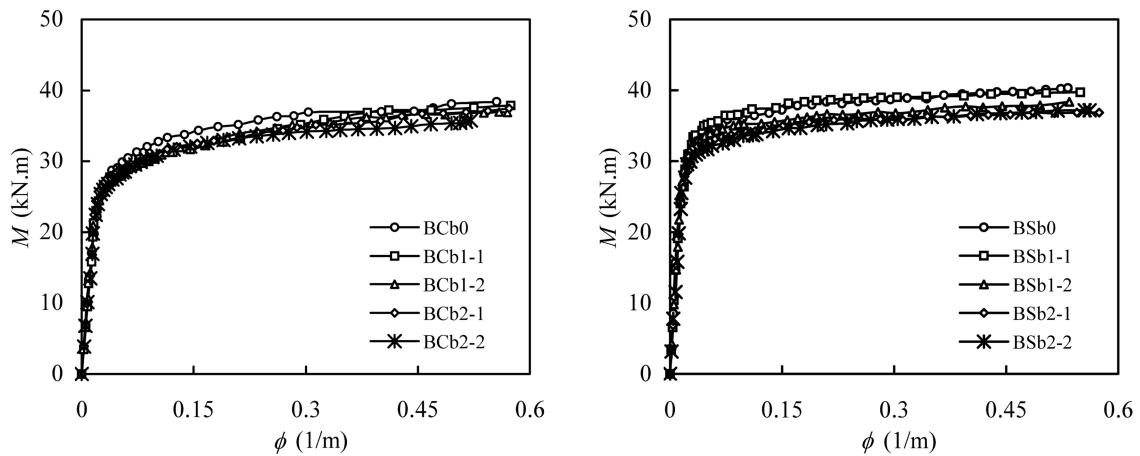
Fig. 14 Moment (M) versus curvature (ϕ) relationships

Fig. 15 Moment versus extreme fibre strains at mid-span of tested beams
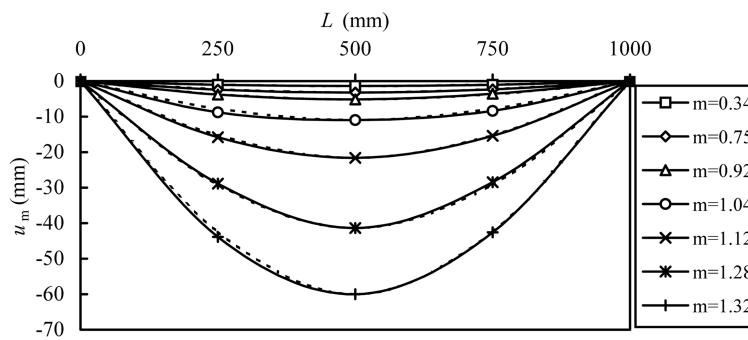
(a) BCb1-1
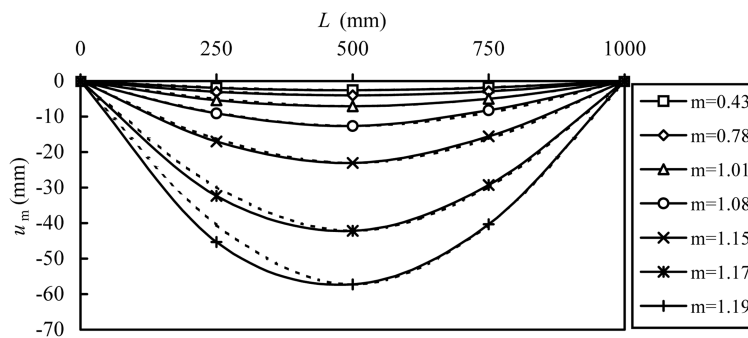
(b) BSb1-1

Fig. 16 Typical deflection curves of tested beams

zone and the buckles are distributed equally and symmetrically. The failure mode of core concrete is crushing at the place of local buckling of the compressive steel plate. The measured bending moment versus mid-span deflections and bending moment versus curvatures are given in Figs. 13 and 14. The moment versus curvature diagrams show that there is an initial elastic response, then inelastic

behaviour with gradually decreasing stiffness, until the ultimate moment is reached asymptotically. It was found that after the fibre tensile strain reaches $10000\,\mu\varepsilon$, the moment tends to stabilize. For practical considerations, the moment corresponding to the maximum fibre tensile strain of $10000\,\mu\varepsilon$ was defined as the ultimate bending moment capacity (M_{ue}) of the composite beam (Han 2004). The ultimate bending moment capacities (M_{ue}) of the current specimens determined are listed in Table 2. The measured bending moment versus extreme fibre compressive and tensile strains are shown in Fig. 15.

A careful examination of the test results revealed that, in general, the moment versus curvature relationship goes into an inelastic stage at 20% of the ultimate bending moment capacity (M_{ue}), so the initial section flexural stiffness (K_{ie}) was defined as the secant stiffness corresponding to a moment of 0.2 M_{ue}. The moment versus curvature response was also used to determine the serviceability-level section flexural stiffness (K_{se}). K_{se} was defined as the secant stiffness corresponding to the serviceability-level moment of 0.6 M_{ue} (Varma 2002). The initial section flexural stiffness (K_{ie}) and the serviceability-level section flexural stiffness (K_{se}) of the tested specimens so determined were listed in Table 2.
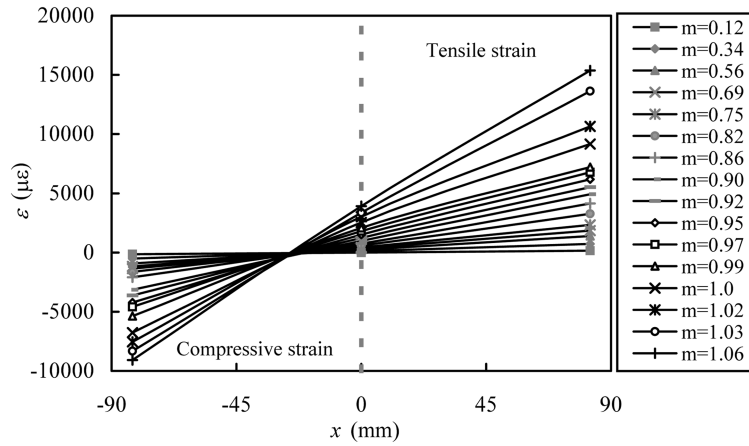
(a) BCb1-1
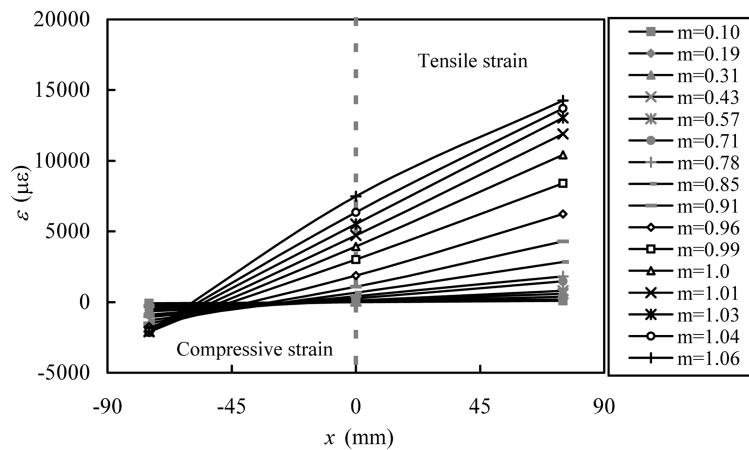
(b) BSb1-1

Fig. 17 Typical distribution of strains across the mid-span section

Because of the concrete infill, the tested beam specimens behaved in a relatively ductile manner and testing proceeded in a smooth and controlled way. During the test, the deflection curve was approximately in the shape of a half sine wave. Specimens BCb1-1 and BSb1-1 were selected to illustrate the deflection development of the composite beams with different moment level (m), shown in Fig. 16, where the ratio of m is given by M/M_{ue}. The sinusoids with the same values in the middle span were also shown in Fig. 16 using dashed lines.

The cross-section almost remains plane during the test, specimens BCb1-1 and BSb1-1 are also selected to illustrate the compressive strain, tensile strain and centroid axes strain development of the composite beams with different moment level (m), shown in Fig. 17, in which x represents the position of longitudinal strain gauges at the mid-span section.

2.3. Scanning electron microscopy (SEM) tests

In order to investigate the characteristics of different core concrete of CFST and RACFST specimens, the microstructures of a few selected failure test specimens were studied by scanning electron microscopy (SEM). Figs. 18(a), (b) and (c) show the SEM micrographs of normal concrete, RAC with 25% and 50% RCA respectively. It can be seen from these figures that, for normal concrete, the hydration progress has not been completed, and the normal concrete has a more dense microstructures
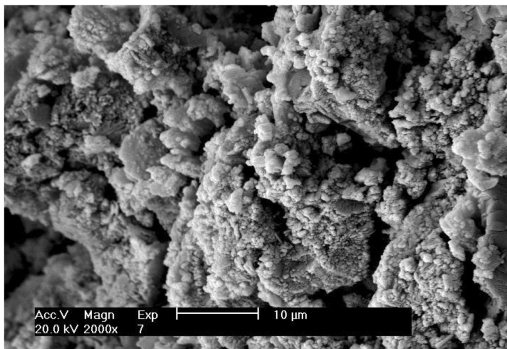
(a) Normal concrete
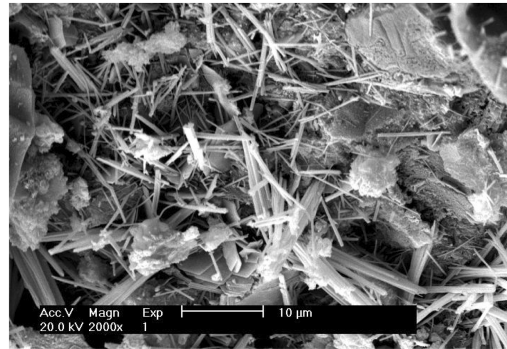
(b) RAC with 25% RCA
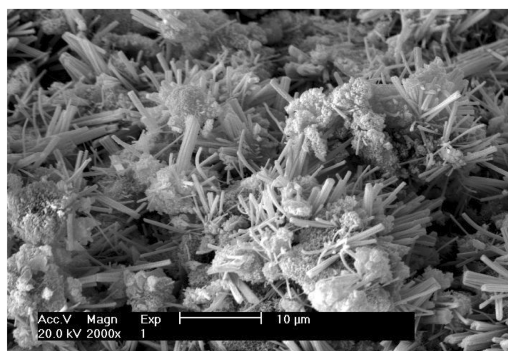
(c) RAC with 50% RCA

Fig. 18 SEM micrographs of different core concrete

than that of the RAC. The RAC has a more reticular and porous microtexture compared to the normal concrete, and the higher the RCA replacement ratio is, the more obvious of the reticular and porous microtexture is. The relatively more porous appearance of the RAC and the reticular microtexture of hydrates formed may possibly explain the reduction in the bearing capability and stiffness of RACFST specimens compared to the corresponding CFST specimens.

3. Analysis of test results and discussion

3.1. Type I: Stub column tests

For convenience of comparisons of the elastic modulus (E_{sc}) and ultimate strength (N_{ue}) of the stub columns under different RCA replacement ratio, the elastic modulus loss index (*ELI*) and strength loss index (*SLI*) as following are defined:

$$ELI = \frac{E_{sc0} - E_{sc1}(\text{or } E_{sc2})}{E_{sc0}} \tag{1}$$

$$SLI = \frac{N_{ue0} - N_{ue1}(\text{or} N_{ue2})}{N_{ue0}} \tag{2}$$

where, E_{sc0} and N_{ue0} are the elastic modulus and ultimate strengths of the specimens with normal concrete; E_{sc1} (E_{sc2}) and N_{ue1} (N_{ue2}) are the elastic modulus and ultimate strengths of the specimens with RAC containing 25% (50%) RCA.

The elastic modulus loss index (*ELI*) and strength loss index (*SLI*) so determined were listed in Table 1, in the calculations, E_{sc1} (N_{ue1}) and E_{sc2} (N_{ue2}) were taken as the average value of the elastic modulus (ultimate strength) of the tested specimens.

Figs. 19 and 20 show the influences of RCA replacement ratio on the elastic modulus and ultimate strengths of stub columns respectively, where NC represents the specimens with normal concrete and 25% RCA (50% RCA) represents the specimens with RAC containing 25% (50%) RCA. It can be seen that, generally, the elastic modulus and ultimate strengths of the specimens with RAC are lower than those of the specimens with normal concrete.

(a) Concrete filled CHS   (b) Concrete filled SHS
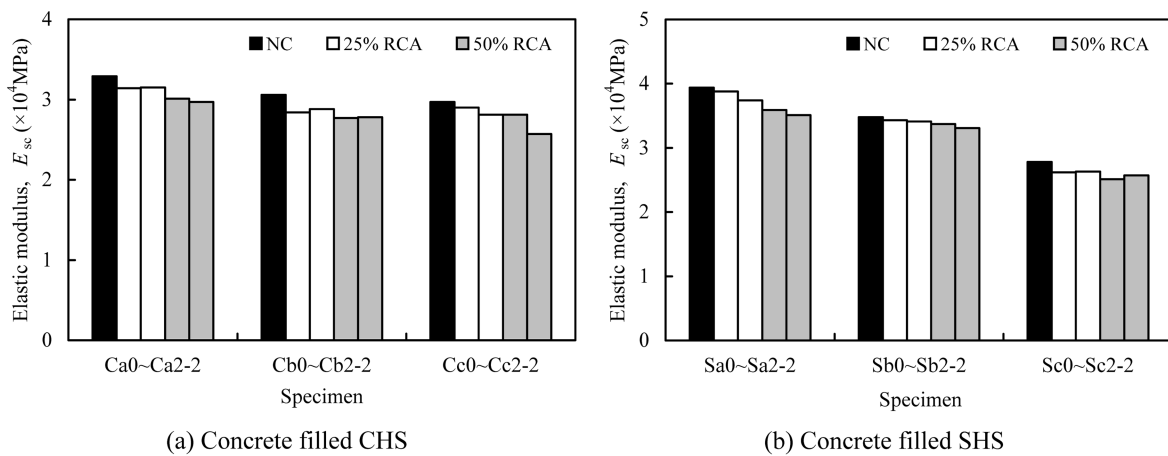
Fig. 19 Influences of RCA replacement ratio on the elastic modulus of stub columns

The results in Table 1 illustrate that the elastic modulus of the specimens with normal concrete are 2.2% to 5.4%, and 4.8% to 9.1% higher than those of columns with RAC containing 25% RCA and 50% RCA respectively. The ultimate strengths of the specimens with normal concrete are 1% to 5%, and 2.4% to 9.4% higher than those of columns with RAC containing 25% RCA and 50% RCA respectively. And at the same time, the elastic modulus and compressive mean cube strength of normal concrete are 5.1% to 10.5%, and 2.1% to 14.3% higher than those of RAC containing 25% RCA and 50% RCA respectively. The lowering in the elastic modulus and ultimate strength of RAC in-fill columns can be attributed to the lower elastic modulus and strength of RAC as compared to the normal concrete.

One of the parameters used to quantify section ductility is the ductility index (*DI*). The definition given in Han (2002) is adopted in this paper. It is expressed as

$$DI = \frac{\varepsilon_{85\%}}{\varepsilon_{ue}} \qquad (3)$$

where, ε_{ue} is the strain at the ultimate strength, and $\varepsilon_{85\%}$ is the strain when the load falls to 85% of the ultimate strength.

For circular specimens, the post-peak loads are all higher than 85% of the ultimate strength till the maximum strain ($\varepsilon_{max} = 0.4$). So the ductility indexes (*DI*) so determined are plotted in Fig. 21 against the RCA replacement ratio only for square specimens. It can be seen from Fig. 21 that, in general, the ductility index increases with the increase in RCA replacement ratio. At the same time, it can be concluded that a greater reduction of ductility for SHS specimens occurs. The reasons are that the constraining effect of circular steel tube to core concrete is better than that of square steel tube for CFST member with the same confinement factor (ξ) and SHS specimens are more prone to local buckling than CHS specimens.

A strength index (*SI*) is defined to quantify the section strength. It is expressed as

$$SI = \frac{N_{ue}}{N_{uo}} \qquad (4)$$

(a) Concrete filled CHS   (b) Concrete filled SHS
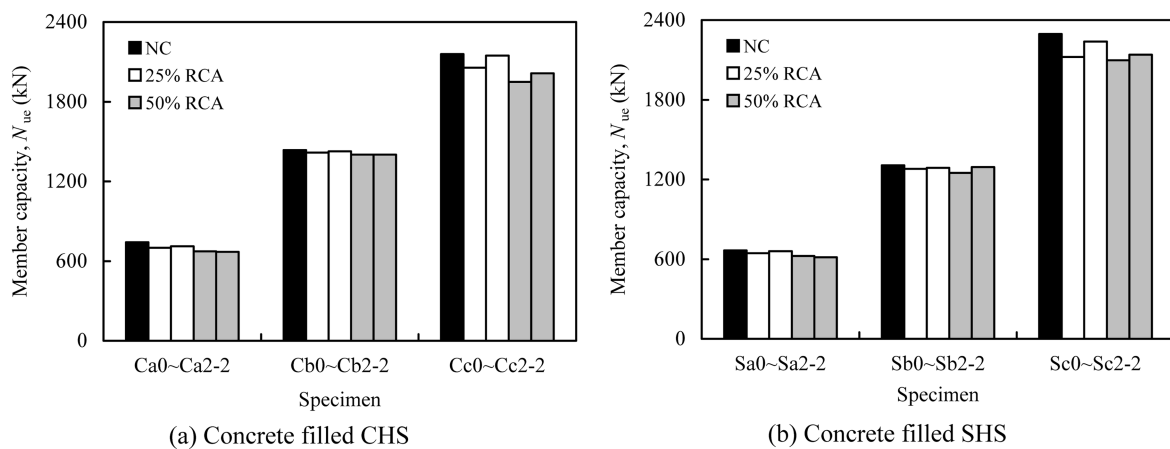
Fig. 20 Influences of RCA replacement ratio on the ultimate strengths of stub columns
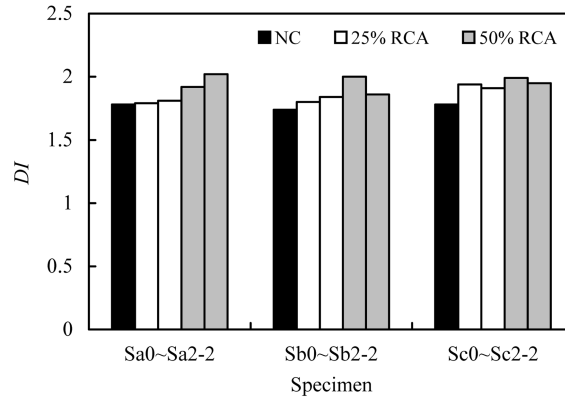
Fig. 21 Influences of RCA replacement ratio on the ductility index of square stub columns

(a) Concrete filled CHS   (b) Concrete filled SHS
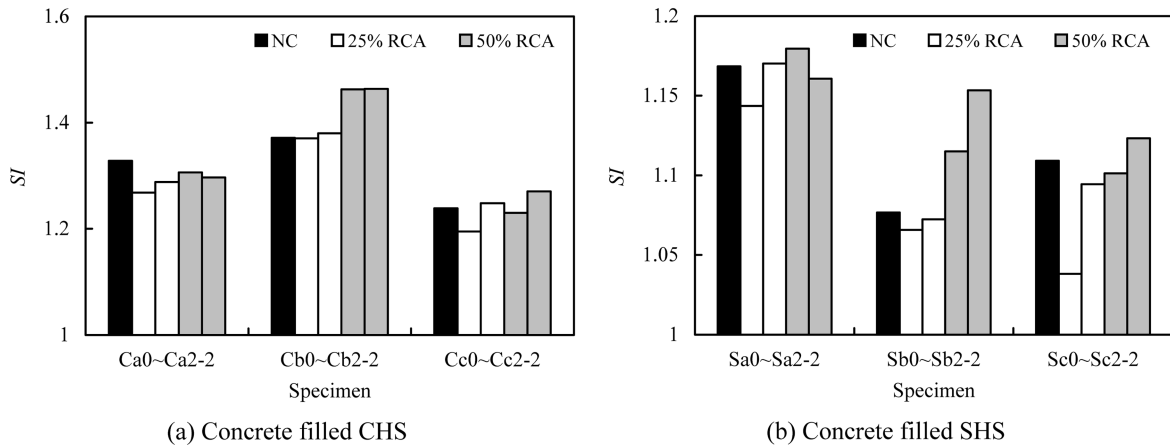
Fig. 22 *SI* versus RCA replacement ratio relationships of stub columns

where N_{uo} $(=A_s \cdot f_{sy} + 0.85A_c \cdot f_c)$ is the sectional capacity as in ACI318-99 (1999), f_c is the specified compressive cylinder strength of concrete.

The strength indexes (*SI*) so determined are plotted in Fig. 22 against the RCA replacement ratio. It can be seen from Fig. 22 that the influence of RCA replacement ratio is moderate.

The ultimate strengths of stub columns with the RAC predicted using the following six design methods are compared with the current test results:

- ACI 318-99 (1999)
- AIJ (1997)
- AISC-LRFD (1999)
- BS5400 (1979)
- DBJ13-51-2003 (2003)
- EC4 (1994)

In all design calculations, the material partial safety factors were set to unity.

Predicted ultimate strengths (N_{uc}) using different methods are compared with test results (N_{ue}) in

Table 7 Comparison between predicted member capacities and test results (stub columns)

No.	Specimen	N_{ue} (kN)	ACI 318-99 (1999)		AIJ (1997)		AISC-LRFD (1999)		BS5400 (1979)		DBJ13-51-2003 (2003)		EC4 (1994)	
			N_{uc} (kN)	$\frac{N_{uc}}{N_{ue}}$	N_{uc} (kN)	$\frac{N_{uc}}{N_{ue}}$	N_{uc} (kN)	$\frac{N_{uc}}{N_{ue}}$	N_{uc} (kN)	$\frac{N_{uc}}{N_{ue}}$	N_{uc} (kN)	$\frac{N_{uc}}{N_{ue}}$	N_{uc} (kN)	$\frac{N_{uc}}{N_{ue}}$
1	Ca1-1	700	533	0.761	603	0.861	529	0.756	779	1.113	611	0.873	701	1.001
2	Ca1-2	711	533	0.750	603	0.848	529	0.744	779	1.096	611	0.859	701	0.986
3	Ca2-1	674	497	0.737	567	0.841	494	0.733	746	1.107	570	0.846	662	0.982
4	Ca2-2	669	497	0.743	567	0.848	494	0.738	746	1.115	570	0.852	662	0.990
5	Cb1-1	1417	1034	0.730	1155	0.815	1027	0.725	1466	1.035	1171	0.826	1345	0.949
6	Cb1-2	1427	1034	0.725	1155	0.809	1027	0.720	1466	1.027	1171	0.821	1345	0.943
7	Cb2-1	1401	958	0.684	1080	0.771	952	0.680	1396	0.996	1086	0.775	1261	0.900
8	Cb2-2	1402	958	0.683	1080	0.770	952	0.679	1396	0.996	1086	0.775	1261	0.899
9	Cc1-1	2055	1720	0.837	1904	0.927	1708	0.831	2375	1.156	1934	0.941	2216	1.078
10	Cc1-2	2147	1720	0.801	1904	0.887	1708	0.796	2375	1.106	1934	0.901	2216	1.032
11	Cc2-1	1950	1585	0.813	1769	0.907	1575	0.808	2250	1.154	1784	0.915	2067	1.060
12	Cc2-2	2014	1585	0.787	1769	0.878	1575	0.782	2250	1.117	1784	0.886	2067	1.026
	Mean Value			0.754		0.847		0.749		1.085		0.856		0.987
	COV (Coefficient of Variation)			0.048		0.05		0.048		0.057		0.052		0.057
1	Sa1-1	645	564	0.874	564	0.874	561	0.870	556	0.862	602	0.933	612	0.949
2	Sa1-2	660	564	0.855	564	0.855	561	0.850	556	0.842	602	0.912	612	0.927
3	Sa2-1	624	529	0.848	529	0.848	527	0.845	524	0.840	561	0.899	571	0.915
4	Sa2-2	614	529	0.862	529	0.862	527	0.858	524	0.853	561	0.914	571	0.930
5	Sb1-1	1279	1200	0.938	1200	0.938	1194	0.934	1182	0.924	1292	1.010	1307	1.022
6	Sb1-2	1287	1200	0.932	1200	0.932	1194	0.928	1182	0.918	1292	1.004	1307	1.016
7	Sb2-1	1250	1121	0.897	1121	0.897	1116	0.893	1109	0.887	1199	0.959	1214	0.971
8	Sb2-2	1293	1121	0.867	1121	0.867	1116	0.863	1109	0.858	1199	0.927	1214	0.939
9	Sc1-1	2123	2045	0.963	2045	0.963	2035	0.959	2012	0.948	2208	1.040	2236	1.053
10	Sc1-2	2238	2045	0.914	2045	0.914	2035	0.909	2012	0.899	2208	0.987	2236	0.999
11	Sc2-1	2098	1905	0.908	1905	0.908	1896	0.904	1883	0.898	2043	0.974	2071	0.987
12	Sc2-2	2140	1905	0.890	1905	0.890	1896	0.886	1883	0.880	2043	0.955	2071	0.968
	Mean Value			0.896		0.896		0.892		0.884		0.960		0.973
	COV (Coefficient of Variation)			0.036		0.036		0.036		0.035		0.044		0.043

Table 7 for specimens with circular and square sections.

Results in Table 7 show that both ACI318-99, AIJ, AISC-LRFD, DBJ13-51-2003 and EC4 are conservative for predicting the ultimate strengths of the specimens with circular sections. Overall, ACI 318-99 and AISC-LRFD give the ultimate strengths about 25% lower than the results obtained in the tests. AIJ and DBJ13-51-2003 give the ultimate strength about 15% lower than the measured results. However, BS5400 gives an ultimate strength about 9% higher than the test results, gives an unsafe prediction.

Overall, the proposed method of EC4, which gives a mean of 0.987 and a COV of 0.057 respectively, is the best predictor to predict the ultimate strength of circular HSS columns filled with RAC containing RCA less than 50%.

Results in Table 7 clearly show that all design methods are conservative for predicting the ultimate strengths of the specimens with square sections. Overall, ACI318-99, AIJ, AISC-LRFD and BS5400 give the ultimate strength about 10% to 12% lower than the results obtained in the tests. The design methods proposed by DBJ13-51-2003 predicted a slightly lower strength than the test result. Overall, the proposed method of EC4, which gives a mean of 0.973 and a COV of 0.043 respectively, is the best predictor to predict the ultimate strength of square HSS columns filled with RAC containing RCA less than 50%.

3.2. Type II: Beam tests

To account for the influences of different filling concrete, the stiffness loss index (SLI_i or SLI_s) and moment loss index (MLI) as following are defined:

$$SLI_i = \frac{K_{ie0} - K_{ie1}(\text{or } K_{ie2})}{K_{ie0}} \tag{5}$$

$$SLI_s = \frac{K_{se0} - K_{se1}(\text{or } K_{se2})}{K_{se0}} \tag{6}$$

$$MLI = \frac{M_{ue0} - M_{ue1}(\text{or } M_{ue2})}{M_{ue0}} \tag{7}$$

where K_{ie0}, K_{se0} and M_{ue0} are the initial section flexural stiffness, serviceability-level section flexural stiffness and ultimate bending moments of the specimens with normal concrete; $K_{ie1}(K_{ie2})$, $K_{se1}(K_{se2})$ and M_{ue1} (M_{ue2}) are the initial section flexural stiffness, serviceability-level section flexural stiffness and ultimate bending moments of the specimens with RAC containing 25% (50%) RCA.

Figs. 23, 24 and 25 are the influences of RCA replacement ratio on the initial section flexural stiffness, serviceability-level section flexural stiffness and ultimate bending moments of the specimens

(a) Concrete filled CHS   (b) Concrete filled SHS
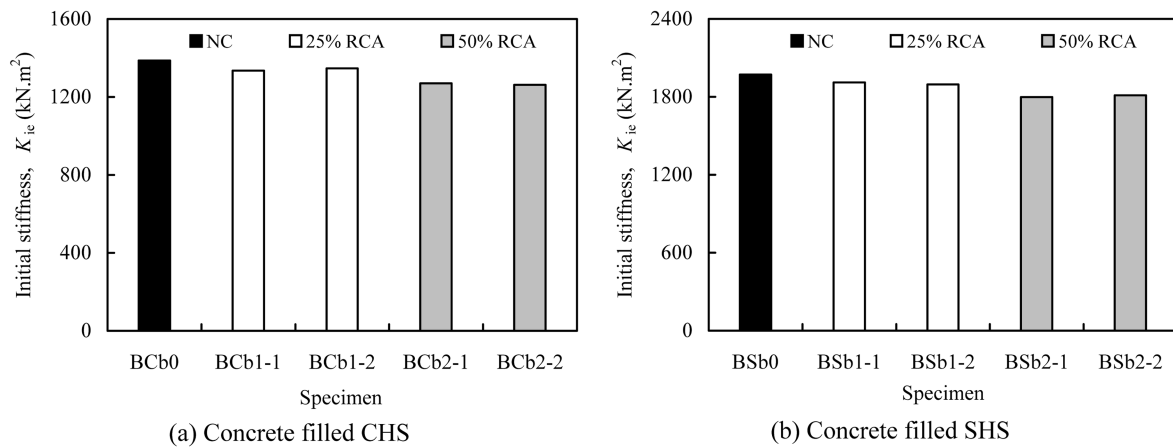
Fig. 23 Influences of RCA replacement ratio on the initial section flexural stiffness

respectively. It also can be seen that, generally, the initial section flexural stiffness, serviceability-level section flexural stiffness and ultimate bending moments of the specimens with normal concrete are higher than those of the specimens with RAC. The lowering in the flexural stiffness and ultimate bending moment of RAC in-fill specimens also can be attributed to the lower elastic modulus and strength of RAC as compared to the normal concrete.

The stiffness loss index (SLI_i or SLI_s) and moment loss index (MLI) so determined are listed in Table 2, in the calculations, $K_{ie1}(K_{ie2})$, $K_{se1}(K_{se2})$ and $M_{ue1}(M_{ue2})$ are taken as the average value of the tested values. It can be found from Table 2 that the initial section flexural stiffness and serviceability-level section flexural stiffness of the specimens with RAC containing less than 50% RCA were 3.3% to 8.7%, and 3.1% to 8.2% lower than those of specimens with normal concrete. The ultimate bending moments of the specimens with normal concrete were 3.5% to 8.1% higher than those of beams with RAC containing less than 50% RCA.

The initial section flexural stiffness, serviceability-level section flexural stiffness and bending

(a) Concrete filled CHS   (b) Concrete filled SHS
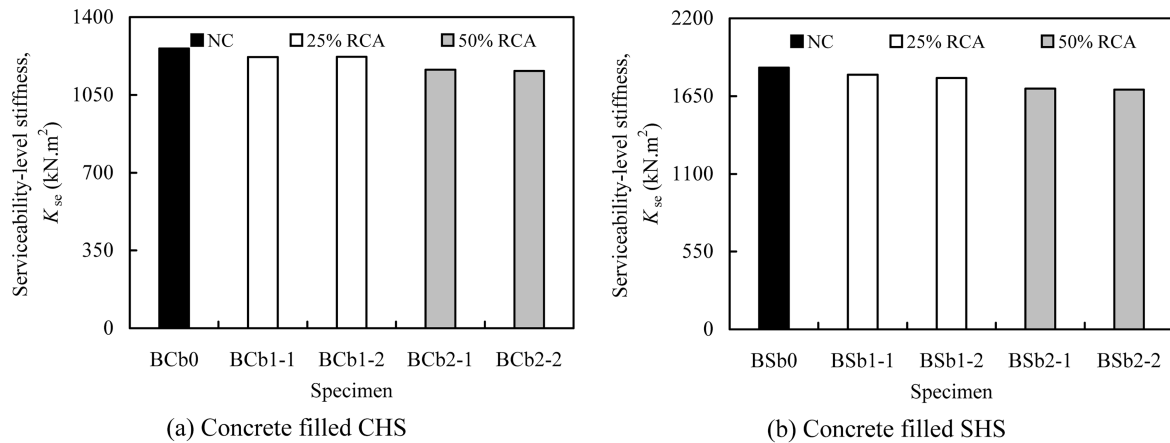
Fig. 24 Influences of RCA replacement ratio on the serviceability-level section flexural stiffness

(a) Concrete filled CHS   (b) Concrete filled SHS
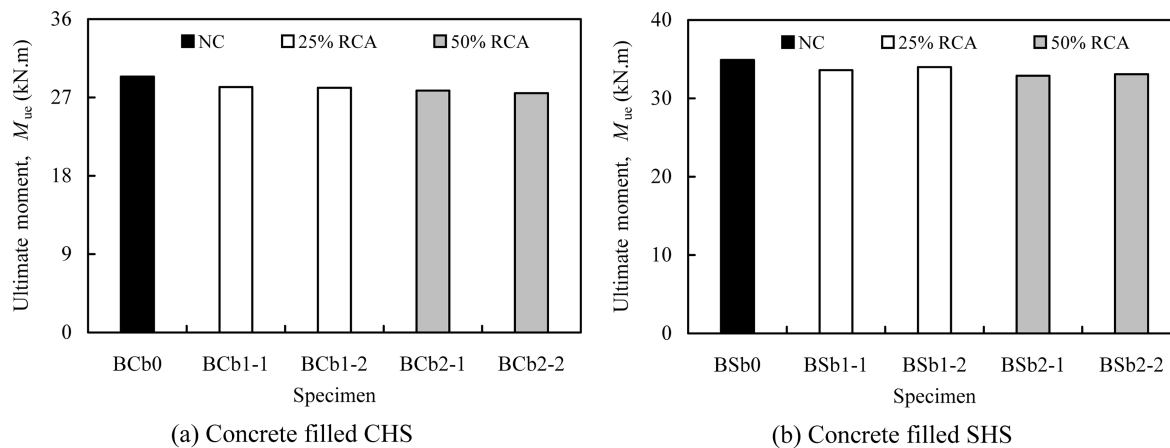
Fig. 25 Influences of RCA replacement ratio on the ultimate bending moment of tested beams

Table 8 Comparison between predicted initial section flexural stiffness and test results

No.	Specimen	K_{ie} (kN.m²)	ACI 318-99 (1999) K_{ic} (kN.m²)	$\frac{K_{ic}}{K_{ie}}$	AIJ (1997) K_{ic} (kN.m²)	$\frac{K_{ic}}{K_{ie}}$	AISC-LRFD (1999) K_{ic} (kN.m²)	$\frac{K_{ic}}{K_{ie}}$	BS5400 (1979) K_{ic} (kN.m²)	$\frac{K_{ic}}{K_{ie}}$	DBJ13-51-2003 (2003) K_{ic} (kN.m²)	$\frac{K_{ic}}{K_{ie}}$	EC4 (1994) K_{ic} (kN.m²)	$\frac{K_{ic}}{K_{ie}}$
1	BCb1-1	1335.3	1042	0.780	1068	0.800	1574	1.179	1494	1.119	1737	1.301	1527	1.144
2	BCb1-2	1347.1	1042	0.774	1068	0.793	1574	1.168	1494	1.109	1737	1.289	1527	1.134
3	BCb2-1	1270.3	1030	0.811	1056	0.831	1527	1.202	1419	1.117	1706	1.343	1504	1.184
4	BCb2-2	1262.1	1030	0.816	1056	0.837	1527	1.210	1419	1.124	1706	1.352	1504	1.192
	Mean Value			0.795		0.815		1.190		1.117		1.321		1.164
	COV (Coefficient of Variation)			0.021		0.022		0.020		0.006		0.031		0.029
1	BSb1-1	1911.5	1445	0.756	1483	0.776	2042	1.068	1961	1.026	1997	1.045	1998	1.045
2	BSb1-2	1896.1	1445	0.762	1483	0.782	2042	1.077	1961	1.034	1997	1.053	1998	1.054
3	BSb2-1	1798.5	1432	0.796	1470	0.817	1989	1.106	1877	1.044	1970	1.095	1972	1.096
4	BSb2-2	1811.3	1432	0.791	1470	0.812	1989	1.098	1877	1.036	1970	1.088	1972	1.089
	Mean Value			0.776		0.797		1.087		1.035		1.070		1.071
	COV (Coefficient of Variation)			0.020		0.021		0.018		0.007		0.025		0.025

Table 9 Comparison between predicted serviceability-level section flexural stiffness and test results

No.	Specimen	K_{se} (kN.m²)	ACI 318-99 (1999) K_{sc} (kN.m²)	$\frac{K_{sc}}{K_{se}}$	AIJ (1997) K_{sc} (kN.m²)	$\frac{K_{sc}}{K_{se}}$	AISC-LRFD (1999) K_{sc} (kN.m²)	$\frac{K_{sc}}{K_{se}}$	BS5400 (1979) K_{sc} (kN.m²)	$\frac{K_{sc}}{K_{se}}$	DBJ13-51-2003 (2003) K_{sc} (kN.m²)	$\frac{K_{sc}}{K_{se}}$	EC4 (1994) K_{sc} (kN.m²)	$\frac{K_{sc}}{K_{se}}$
1	BCb1-1	1219.8	1042	0.854	1068	0.876	1574	1.290	1494	1.225	1737	1.424	1527	1.252
2	BCb1-2	1221.6	1042	0.853	1068	0.874	1574	1.288	1494	1.223	1737	1.422	1527	1.250
3	BCb2-1	1163.1	1030	0.886	1056	0.908	1527	1.313	1419	1.220	1706	1.467	1504	1.293
4	BCb2-2	1157.9	1030	0.890	1056	0.912	1527	1.319	1419	1.225	1706	1.473	1504	1.299
	Mean Value			0.871		0.893		1.303		1.223		1.447		1.274
	COV (Coefficient of Variation)			0.020		0.020		0.016		0.002		0.027		0.026
1	BSb1-1	1801.5	1445	0.802	1483	0.823	2042	1.133	1961	1.089	1997	1.109	1998	1.109
2	BSb1-2	1779.1	1445	0.812	1483	0.834	2042	1.148	1961	1.102	1997	1.122	1998	1.123
3	BSb2-1	1702.3	1432	0.841	1470	0.864	1989	1.168	1877	1.103	1970	1.157	1972	1.158
4	BSb2-2	1695.5	1432	0.845	1470	0.867	1989	1.173	1877	1.107	1970	1.162	1972	1.163
	Mean Value			0.825		0.847		1.156		1.100		1.138		1.138
	COV (Coefficient of Variation)			0.021		0.022		0.018		0.008		0.026		0.026

moment of the specimens with the RAC predicted using the aforementioned six design methods are compared with those obtained in the current tests in Tables 8, 9 and 10.

In all design calculations, the material partial safety factors were set to unity.

Table 10 Comparison between predicted ultimate bending moments and test results (beams)

No. Specimen	M_{ue} (kN.m)	ACI 318-99 (1999)		AIJ (1997)		AISC-LRFD (1999)		BS5400 (1979)		DBJ13-51-2003 (2003)		EC4 (1994)	
		M_{uc} (kN.m)	$\dfrac{M_{uc}}{M_{ue}}$	M_{uc} (kN.m)	$\dfrac{M_{uc}}{M_{ue}}$	M_{uc} (kN.m)	$\dfrac{M_{uc}}{M_{ue}}$	M_{uc} (kN.m)	$\dfrac{M_{uc}}{M_{ue}}$	M_{uc} (kN.m)	$\dfrac{M_{uc}}{M_{ue}}$	M_{uc} (kN.m)	$\dfrac{M_{uc}}{M_{ue}}$
1 BCb1-1	28.8	30	1.042	23.3	0.809	23.3	0.809	27.4	0.951	25.4	0.882	28.4	0.986
2 BCb1-2	28.7	30	1.045	23.3	0.812	23.3	0.812	27.4	0.955	25.4	0.885	28.4	0.990
3 BCb2-1	27.8	29.7	1.068	23.3	0.838	23.3	0.838	27.1	0.975	24.8	0.892	28	1.007
4 BCb2-2	27.5	29.7	1.080	23.3	0.847	23.3	0.847	27.1	0.985	24.8	0.902	28	1.018
Mean Value			1.059		0.827		0.827		0.967		0.890		1.000
COV (Coefficient of Variation)			0.018		0.019		0.019		0.016		0.009		0.015
1 BSb1-1	33.6	27.5	0.818	21.9	0.652	21.9	0.652	25.2	0.750	23.4	0.696	26.1	0.777
2 BSb1-2	34.0	27.5	0.809	21.9	0.644	21.9	0.644	25.2	0.741	23.4	0.688	26.1	0.768
3 BSb2-1	32.9	27.1	0.824	21.9	0.666	21.9	0.666	25.2	0.766	23	0.699	25.8	0.784
4 BSb2-2	33.1	27.1	0.819	21.9	0.662	21.9	0.662	25.2	0.761	23	0.695	25.8	0.779
Mean Value			0.818		0.656		0.656		0.755		0.695		0.777
COV (Coefficient of Variation)			0.006		0.010		0.010		0.011		0.005		0.007

Results in Table 8 show that both AISC-LRFD, BS5400, DBJ13-51-2003 and EC4 give an unsafe prodiction for the initial section flexural stiffness of the specimens with different filling concrete. For circular specimens, DBJ13-51-2003 is the most unsafe one and gives a predicting results about 32% higher than the test ones. AISC-LRFD, BS5400 and EC4 give the predicting results about 19%, 12% and 16% higher than the test results respectively. Overall, ACI318-99 and AIJ give the predicting results about 20% and 18% lower than the results obtained in the tests respectively. For square specimens, AISC-LRFD is the most unsafe one and gives a predicting results about 9% higher than the test results. BS5400, DBJ13-51-2003 and EC4 give the predicting results about 4%, 7% and 7% higher than the test results respectively. Overall, ACI318-99 and AIJ give the predicting results about 22% and 20% lower than the results obtained in the tests respectively.

Results in Table 9 also show that both AISC-LRFD, BS5400, DBJ13-51-2003 and EC4 give an unsafe prodiction for the serviceability-level section flexural stiffness. For circular specimens, DBJ13-51-2003 is the most unsafe one and gives a prediction about 45% higher than the test results. AISC-LRFD, BS5400 and EC4 give the prediction about 30%, 22% and 27% higher than the test result respectively. ACI318-99 and AIJ give the predictions about 13% and 11% lower than the test results. For square specimens, AISC-LRFD is the most unsafe one and gives a prediction about 16% higher than the test results. BS5400, DBJ13-51-2003 and EC4 give the predictions about 10%, 14% and 14% higher than the test results respectively. Overall, ACI318-99 and AIJ give the predictions about 18% and 15% lower than the test results.

Results in Table 10 clearly show that both AIJ, AISC-LRFD, BS5400 and DBJ13-51-2003 are conservative for predicting the ultimate bending moments of circular specimens. AIJ, AISC-LRFD and DBJ13-51-2003 give the predicting results about 11% to 17% lower than the test ones. However, ACI318-99 gives a prediction about 6% higher than these of the measured results, is an unsafe

predictor. Overall, the proposed method by EC4 gives a mean of 1.000 and a COV of 0.015 respectively, is the best predictor to predict the ultimate bending moment of circular HSS columns filled with RAC containing less than 50% RCA. However, all design methods are conservative for predicting the ultimate bending moments of the specimens with square sections. AIJ, AISC-LRFD and DBJ13-51-2003 give the predicting results about 30% to 34% lower than the tested ultimate bending moments. The predicting results of BS5400 and EC4 are about 25% and 22% lower than the tested ultimate bending moments respectively. Overall, the proposed method by ACI318-99, which gives a mean of 0.818 and a COV of 0.006 respectively, is the best predictor to predict the ultimate bending moment of square HSS columns filled with RAC containing RCA less than 50%.

4. Conclusions

The behaviour of HSS stub columns and beams filled with normal concrete and recycled aggregate concrete under instantaneous loading was investigated experimentally. Based on the results of this study, the following conclusions can be drawn within the scope of these tests:

(1) The compressive and flexural behaviour of RACFST are similar to the corresponding HSS columns filled with normal concrete.

(2) The ultimate strength of stub columns with normal concrete are 1% to 5%, and 2.4% to 9.4% higher than that of the specimens with RAC containing 25% RCA and 50% RCA respectively, for the elastic modulus, the ranges are 2.2% to 5.4%, and 4.8% to 9.1%.

(3) The initial section flexural stiffness and serviceability-level section flexural stiffness of the beams with the RAC were 3.3% to 8.7%, and 3.1% to 8.2% lower than those of the beams with normal concrete. The bending moment of the specimens with normal concrete was 3.5% to 8.1% higher than that of beams with RAC.

(4) The loading capacity of RACFST stub columns and beams can be conservatively predicted by using AIJ, AISC-LRFD, DBJ13-51-2003 and EC4 recommendations and the EC4 method gives closer predictions of the test results than other method.

Acknowledgements

References

ACI 318-99 (1999), "Building code requirements for structural concrete and commentary", Farmington Hills (MI), American Concrete Institute, Detroit, U.S.A.
AIJ (1997), "Recommendations for design and construction of concrete filled steel tubular structures", Architectural Institute of Japan, Tokyo, Japan.

AISC-LRFD (1999), "Load and resistance factor design specification for structural steel buildings", 2nd ed., American Institute of Steel Construction (AISC), Chicago, U.S.A.

Ajdukiewicz, A. and Kliszczewicz, A. (2002), "Influences of recycled aggregates on mechanical properties of HS/HPC", *Cement & Concrete Composites*, **24**(2), 269-279.

ASCCS. (1997), "Concrete filled steel tubes-A comparison of international codes and practices", ASCCS Seminar, Innsbruck, Austria.

BS5400: Part 5 (1979), "Concrete and composite bridges", British Standard Institute.

DBJ 13-51-2003 (2003), "Technical specification for concrete-filled steel tubular structures", Fuzhou (in Chinese).

Eurocode 4 (1994), "Design of composite steel and concrete structures, Part1.1: General rules and rules for buildings (together with United Kingdom National Application Document)", DD ENV 1994-1-1, British Standards Institution, London W1A2BS.

Han, L. H. (2002), "Tests on stub columns of concrete-filled RHS sections", *J. Constr. Steel Res.*, **58**(3), 353-372.

Han, L. H. (2004), "Flexural behaviour of concrete-filled steel tubes", *J. Constr. Steel Res.*, **60**(2), 313-337.

Han, L. H., Zhao, X. L. and Tao, Z. (2001), "Tests and mechanics model of concrete-filled SHS stub columns, columns and beam-columns", *Steel and Composite Structures*, **1**(1), 51-74.

Katz, A. (2003), "Properties of concrete made with recycled aggregate from partically hydrated old concrete", *Cement and concrete Research*, **33**(5), 703-711.

Konno, K., Sato, Y., Kakuta, Y. and Ohira, M. (1997), "Property of recycled concrete column encased by steel tube subjected to axial compression", *Transactions of the Japan Concrete Institute*, **19**(2), 231-238.

Konno, K., Sato, Y., Ueda, T. and Onaga, M. (1998), "Mechanical property of recycled concrete under lateral confinement", *Transactions of the Japan Concrete Institute*, **20**(3), 287-292.

Lu, Y. Q. and Kennedy, D. J. L. (1994), "The flexural behaviour of concrete-filled hollow structural sections", *Canadian Journal of Civil Engineering*, **21**(1), 111-130.

Olorunsogo, F. T. and Padayachee, N. (2002), "Performance of recycled aggregate concrete monitored by durability indexes", *Cement and Concrete Research*, **32**(2), 179-185.

Schneider, S. P. (1998), "Axially loaded concrete-filled steel tubes", *J. Struct. Eng.*, ASCE, **124**(10), 1125-1138.

Topçu, İ. B. and Şengel, S. (2004), "Properties of concretes produced with waste concrete aggregate", *Cement and Concrete Research*, **34**(8), 1307-1312.

Uy, B. (2000), "Strength of concrete filled steel box columns incorporating local buckling", *J. Struct. Eng.*, ASCE, **126**(3), 341-352.

Varma, A. H., Ricles, J. M., Sause, R. and Lu, L. W. (2002), "Seismic behavior and modeling of high-strength composite concrete-filled steel tube (CFT) beam-columns", *J. Constr. Steel Res.*, **58**(5-8), 725-758.

Xiao, J., Sun, Y. and Falkner, H. (2006), "Seismic performance of frame structures with recycled aggregate concrete", *Eng. Struct.*, **28**(1), 1-8.

Notation

A_s	:	Steel cross-sectional area, in mm^2
A_c	:	Concrete cross-sectional area, in mm^2
CFST	:	Concrete filled steel tube
CHS	:	Circular hollow section
D	:	Sectional dimension, in mm
E_c	:	Concrete modulus of elasticity, in MPa
E_s	:	Steel modulus of elasticity, in MPa
E_{sc}	:	Modulus of elasticity of composite stub columns, in MPa
$f_{ck,cube}$	:	Compressive characteristic strength of concrete (= 0.67 $f_{cm,cube}$), in MPa
$f_{cm,cube}$	:	Compressive mean cube strength of concrete, in MPa
f_{sy}	:	Yield strength of steel, in MPa
HSS	:	Hollow structural steel
K_{ie}	:	Initial section flexural stiffness of composite beams, in kN.m^2
K_{se}	:	Serviceability-level section flexural stiffness of composite beams, in kN.m^2
L	:	Length of stub columns and beams, in mm
M_{uc}	:	Predicted ultimate bending moment capacity of the composite beams, in kN.m
M_{ue}	:	Experimental ultimate bending moment capacity of the composite beams, in kN.m
NCA	:	Natural coarse aggregate
N_{uc}	:	Predicted ultimate strength of the stub columns, in kN
N_{ue}	:	Experimental ultimate strength of the stub columns, in kN
R	:	Recycled coarse aggregate replacement ratio
RAC	:	Recycled aggregate concrete
RACFST	:	Recycled aggregate concrete filled steel tube
RCA	:	Recycled coarse aggregate
SHS	:	Square hollow section
t	:	Wall thickness of circular steel tube or the flat part of square steel tube, in mm
u_m	:	Mid-span deflection of the beam, in mm
ε	:	Strain
ϕ	:	Curvature
ξ	:	Confinement factor ($= \dfrac{A_s \cdot f_{sy}}{A_c \cdot f_{ck,cube}}$)

CC